Numerical Computation of Human Interaction with Arbitrarily Oriented Superquadric Loop Antennas in Personal Communications

Wen-Tzu Chen, *Student Member, IEEE*, and Huey-Ru Chuang, *Member, IEEE*

***Abstract*— Loop antennas are widely used in many personal communication systems such as radio pagers. This paper presents results from an extensive numerical simulation of the human interaction with loop antennas. The loop antenna with a superquadric curve, which is able to model the circular, ellipse, square, and rectangular loop is used to model the rectangular loop antenna with rounded corners. The magnetic frill source is used to model the antenna feeding structure. A realistically shaped full-scale human-body model (1.7 m) is constructed. The coupled integral equations (CIE) approach, which consists a Pocklington-type integral equation (PIE) for the loop antenna and a volume electric field integral equation (VEFIE) for the body with mutual coupling terms, are developed to numerically study this electromagnetic (EM) coupling problem. The method of moments (MoM) is employed for numerical solution. Numerical results for the antenna located at the chest pocket and waist-belt levels of the human body with arbitrary loop orientations are presented at 280-MHz VHF paging band. The pager's internal rectangular loop antenna with rounded corners is modeled by a superquadric loop antenna. It is found that the real part of the impedance (radiation resistance) increases about five times and, hence, the antenna ohmic-loss radiation efficiency increases from 4% (in free-space) to 33, 17, and 26% for the x-, y-, and z-oriented loops when proximate to the body. The radiation efficiencies, reduced by the body absorption effect, are 13, 40, and 27% for the x-, y-, and z-oriented loops, respectively. For the y-oriented loop, which is found to be the most suitable for radio-paging communications, it has the highest value of E_θ average power gain (product of the directive gain and the ohmic-loss and body-absorption efficiencies) in the horizontal plane. The computed antenna characteristics influenced by the human body, including the input impedance, antenna patterns, cross-polarization field level, radiation efficiencies, and maximum/minimum and average power gains, are very useful for the antenna/RF design and the link budget consideration of the personal communication systems.**

***Index Terms*—Human factors, loop antennas, mobile communication.**

I. Introduction

In personal wireless communications, the human interaction with the antenna mounted on the portable communicator is one of the most important considerations for the antenna design. Since the portable communicators are usually very close to the human body, the antenna characteristics such as input impedance radiation patterns/polarizations and antenna efficiency are strongly influenced by the nearby body tissue. Several research efforts have been devoted to evaluation of the electromagnetic (EM) interaction between the human body (particularly the head) and the hand-set dipole or monopole antennas [1]–[3]. For the loop antennas, which sometimes are more suitable than dipole-whip antennas for certain mobile and personal communication applications (such as radio paging), the human interaction effect has not been widely reported yet.

Radio paging is a cost-effective solution for altering personnel by transmitting one-way messages or data. The pagers are widely used in wireless communications due to low cost, small size, and low-power consumption. Usually, the internal antennas of a pager is a loop antenna since it has comparatively better performance than dipole-type antennas due to the human-body effect [4]. This is due to the enhancement of the magnetic field by the human body when the pager is in the vicinity of the body. A pager is usually worn on the belt or kept in the chest pocket and may be kept with different orientation with respect to the body. Hence, the pager's antenna is in proximity to and may have different orientations with respect to the human body. It will be shown later that EM-coupling effects of the human body on the antenna performance strongly depend on the orientation of the loop. For the design consideration of the pager antenna, it is important to investigate the antenna characteristics influenced by the human body and the loop orientation. In [5], the body was replaced as a large conducting reflector plane and the image theory was applied to approximately evaluate the characteristics of rectangular antenna. In [6], a numerical model of the head was constructed and the method of moments was applied to analyze the EM-coupling issue. An experiment has been conducted to measure the field-strength sensitivity of the body-worn pager by using a 1.7-m height cylindrical phantom contained the salty water to simulate the human body [7]. It is found that the human body and the body posture would significantly affect the field-strength sensitivity of the pager. This indicated a realistically shaped full-scale human-body model is necessary for the full investigation of this problem. Recently, coupled-integral-equations (CIE)/method-of-moments (MoM) approach has been used to study the detailed EM-coupling effects of a full-scale human-body model on the circular-loop antennas at radio-paging bands [8]. Since the pager's antenna is usually a rectangular loop with round corners, a superquadric loop of which the curve is able to

Manuscript received June 4, 1997; revised March 16, 1998. This work was supported in part by the National Center for Highspeed Computing and the National Science Council of the Republic of China under Grants NCHC-86-03-011 and NSC 87-2218-E-006-054.

The authors are with the Department of Electrical Engineering, National Cheng Kung University, Tainan, Taiwan, 70101 R.O.C.

Publisher Item Identifier S 0018-926X(98)04872-8.

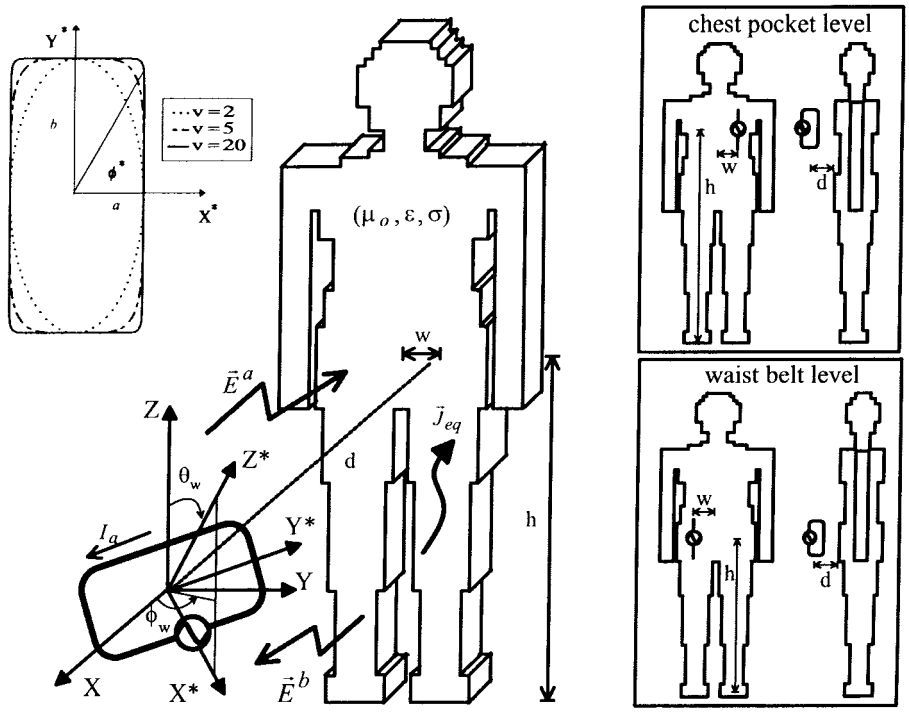

Fig. 1. EM coupling between an arbitrarily oriented superquadric loop antenna and a proximate human-body model at the chest pocket level or the waist belt level.

model the circular, ellipse, square, and rectangular loops is a better model than the circular loop to simulate the pager's antenna.

This paper presents extensive numerical simulation of the human interaction with a superquadric loop antenna, which has arbitrary orientations. The coordinate transformation technique is employed to describe the loop antenna of arbitrary orientation. The CIE/MoM, which consists a Pocklington-type integral equation (PIE) for the superquadric loop antenna and a volume electric field integral equation (VEFIE) for the body with mutual coupling terms, are developed to numerically study this EM-coupling problem. A realistically shaped 3-D man model with a height of 170 cm is used in the numerical simulation. Numerical results at 280-MHz VHF paging band will be presented. The situations of the loop antenna with various orientations in free-space and proximate to the body are studied and compared for radio-paging communication applications. It is noted that although in this analysis the loop antenna is treated as a transmitting antenna, the computed radiation characteristics can also be applied for a receiving antenna. This is from the reciprocity point of view, assuming the human body is a linear and isotropic EM system.

II. Theoretical Analysis and Computational Model

A. A Superquadric Loop Antenna with Arbitrary Orientation

A superquadric loop antenna with arbitrary orientation located near a human body is shown in Fig. 1. Since a pager may be kept in the chest pocket or worn on the waist belt, the two positions of the loop antenna, the pocket level ($d = 2$ cm, $w = 10$ cm, $h = 120$ cm) and the belt level ($d = 2$ cm, $w = -10$ cm, $h = 100$ cm), are considered as shown in Fig. 1. A rotated coordinate frame $X^*Y^*Z^*$ is introduced to describe the arbitrary orientation of a superquadric loop antenna. It can be obtained by the axis rotations of the original coordinate frame XYZ with the Eulerian angles (ϕ_w, θ_w, ψ_w), as shown in Fig. 1. In the coordinate rotation, the angle ψ_w is assumed to be equal to zero. Therefore, the unit vector $\hat{x}^*$ of the new coordinate system is now in the Z-Z^* plane. The unit vector $\hat{z}^*$ is chosen to define the orientation of the superquadric loop antenna and the loop plane coincides with the X^*-Y^* plane. In this case, the parametric expression of a superquadric curve in the X^*-Y^* plane is given by [9], [10]

$$\left|\frac{x^*}{a}\right|^v + \left|\frac{y^*}{b}\right|^v = 1 \tag{1}$$

where a and b are the semi-axis lengths in the X^* and Y^* axis and v is the squareness parameter. The expression of a superquadric curve in (1) has flexibility for modeling circular, ellipse, square, and rectangular thin-wire loop antennas. If $a = b$ and $v = 2$, it is a circular loop. If v is large enough, for example $v = 20$, it is almost a square loop. In Fig. 1 the superquadric curves with various squareness parameters v is also illustrated. An alternative representation of the superquardric loop is given by [9]

$$\begin{cases} x^* = a\psi(\phi^*)\cos\phi^* \\ y^* = b\psi(\phi^*)\sin\phi^* \end{cases} \quad \psi(\phi^*) = \frac{1}{(|\sin\phi^*|^v + |\cos\phi^*|^v)^{1/v}} \quad 0 \le \phi^* \le 2\pi. \tag{2}$$

The differential arc length ds can be expressed in terms of the $d\phi^*$ as in the following:

$$ds^* = (\sqrt{a^2|\sin\phi^*|^{2v-2} + b^2|\cos\phi^*|^{2v-2}})\psi^{v+1}(\phi^*)\,d\phi^* = \Delta(\phi^*)\,d\phi^*. \tag{3}$$

In order to derive the coupling terms in the moment method solution, the expression of the arbitrarily oriented loop in coordinate frame $X^*Y^*Z^*$ is converted to the reference-coordinate form. Using the coordinate transformation technique [11], the position components (x, y, z) are related to (x^*, y^*, z^*) via a coordinate transformation matrix as

$$\begin{bmatrix} x \\ y \\ z \end{bmatrix} = \begin{bmatrix} \cos\theta_w \cos\phi_w & -\sin\phi_w & \sin\theta_w \cos\phi_w \\ \cos\theta_w \sin\phi_w & \cos\phi_w & \sin\theta_w \sin\phi_w \\ -\sin\theta_w & 0 & \cos\theta_w \end{bmatrix} \begin{bmatrix} x^* \\ y^* \\ z^* \end{bmatrix}. \tag{4}$$

Therefore, the representation of a superquardric loop in the reference coordinate frame XYZ can be obtained from (2) and (4). The unit tangential vector $\hat{s}$ on the antenna surface can be expressed in terms of $\hat{x}^*$ and $\hat{y}^*$ [6]. By using the coordinate transformation (4), the expression of $\hat{s}$ in terms of $\hat{x}$, $\hat{y}$, and $\hat{z}$ can be obtained.

B. EM-Coupling Formulation

The electric field $\vec{E}^a$ radiated from the antenna induces an equivalent current density $\vec{J}_{\rm eq}$ inside the human body. The equivalent current density inside a lossy body with parameters $(\sigma, \varepsilon, \mu_o)$ is given by

$$\vec{J}_{\rm eq}(\vec{r}) = [\sigma + j\omega(\varepsilon - \varepsilon_o)]\vec{E}(\vec{r}) = \tau \vec{E}(\vec{r}). \tag{5}$$

The total electric field inside the body is the sum of the incident field radiated from the loop antenna and the body-scattered field determined from the equivalent current density. By using the dyadic Green's function technique, the total electric field inside the body and the loop-antenna current distribution can be formulated as [6], [8]

$$\frac{-1}{j\omega\varepsilon_o}\int_{\rm ant}\left[\hat{s}\cdot\hat{s}' k_o^2 I(s') + \frac{\partial I(s')}{\partial s'}\cdot\frac{\partial}{\partial s}\right] G(s,s')\,ds' - \int_{V_b}\hat{s}\cdot\overleftrightarrow{G}(s,\vec{r}')\cdot\tau(\vec{r}')\vec{E}(\vec{r}')\,dv' = \hat{s}\cdot\vec{E}^i(s) \tag{6}$$

$$\int_{\rm ant} I(s')\hat{s}'\cdot\overleftrightarrow{G}(\vec{r},s')\,ds' + \mathbf{PV}\int_{V_b}\tau(\vec{r}')\vec{E}(\vec{r}')\cdot\overleftrightarrow{G}(\vec{r},\vec{r}')\,dv' - \left[1 + \frac{\tau(\vec{r})}{3j\omega\varepsilon_o}\right]\vec{E}(\vec{r}) = 0 \tag{7}$$

where $\vec{E}^i$ is the impressed field from the antenna feeding source. The magnetic frill is employed to model the loop-antenna feeding structure [12], [13]. The impressed field $\vec{E}^i$ is produced by an annular ring of magnetic current at the feed point. The outer and inner radii of the annular ring are set to the value of $r_o = 2.3r_i$ to model a 50-Ω air-filled coaxial feeding cable having outer radius r_o and inner radius r_i.

C. Moment-Method Solution

Equations (6) and (7) are solved numerically by MoM. The antenna is partitioned into N_a segments and the body is subdivided into N_b cubic cells. The unknown current of the loop antenna is expanded in terms of a set of piecewise sinusoidal basis functions and the induced electric field in the body is approximated by the pulse functions

$$I(\phi^*) = \sum_{n=1}^{N_a} I_n f_n(\phi^*)$$
$$\vec{E}(\vec{r}) = \hat{x}\sum_{n=1}^{N_b} E_x^n p_n(\vec{r}) + \hat{y}\sum_{n=1}^{N_b} E_y^n p_n(\vec{r}) + \hat{z}\sum_{n=1}^{N_b} E_z^n p_n(\vec{r}) \tag{8}$$

where I_n, E_x^n, E_y^n, and E_z^n are the unknown coefficients to be determined. By applying the Galerkin technique and the point-matching technique to (6) and (7), it leads to two sets of simultaneous equations as follows:

$$\begin{aligned}
&\frac{-1}{j\omega\varepsilon_o}\sum_{n=1}^{N_a} I_n \int_{\phi_{m-1}^*}^{\phi_{m+1}^*}\int_{\phi_{n-1}^*}^{\phi_{n+1}^*}\Big\{(s_{x^*}s'_{x^*} + s_{y^*}s'_{y^*}) \times k_o^2 f_n(\phi^{*\prime})\Delta(\phi^{*\prime}) - \frac{(jk_oR+1)}{R^2}[s_{x^*}(x^* - x^{*\prime}) \\
&+ s_{y^*}(y^* - y^{*\prime})]\frac{\partial f_n(\phi^{*\prime})}{\partial\phi^{*\prime}}\Big\} G\cdot f_m(\phi^*)\Delta(\phi^*)\,d\phi^{*\prime}\,d\phi^* \\
&- \sum_{n=1}^{N_b}\sum_{p=1}^{3} E_{x_p}^n \int_{V_b}\tau_n \int_{\phi_{m-1}^*}^{\phi_{m+1}^*}\big[s_x G_{xx_p}(s,r') \\
&+ s_y G_{yx_p}(s,r') + s_z G_{zx_p}(s,r')\big] f_m(\phi^*)\Delta(\phi^*)\,d\phi^*\,dv' \\
&= \int_{\phi_{m-1}^*}^{\phi_{m+1}^*}(s_{x^*}\hat{x}^* + s_{y^*}\hat{y}^*)\cdot\vec{E}^{\,i}(\phi^*) f_m(\phi^*)\Delta(\phi^*)\,d\phi^*
\end{aligned} \tag{9}$$

$$\begin{aligned}
&\sum_{p=1}^{3}\hat{x}_p\Bigg\{\sum_{n=1}^{N_a} I_n\int_{\phi_{n-1}^*}^{\phi_{n+1}^*}\big[G_{x_px}(\vec{r}_i,s')s_x + G_{x_py}(\vec{r}_i,s')s_y \\
&\quad + G_{x_pz}(\vec{r}_i,s')s_z\big] f_n(\phi^{*\prime})\Delta(\phi^{*\prime})\,d\phi^{*\prime} \\
&\quad + \sum_{n=1}^{N_b}\sum_{q=1}^{3} E_{x_q}^n\Bigg[\tau_n\mathbf{PV}\cdot\int_{(\Delta v)_n} G_{x_px_q}(\vec{r}_i,\vec{r}')\,dv' \\
&\quad - \delta_{pq}\delta_{\vec{r}_i\vec{r}_n}\left(1 + \frac{\tau_i}{j3\omega\varepsilon_o}\right)\Bigg]\Bigg\} = 0
\end{aligned} \tag{10}$$

where $m = 1, 2, \cdots, N_a$, $i = 1, 2, \cdots, N_b$, and $G_{x_px_q}$ is the element of the matrix representation for the Dyadic Green's function $\overleftrightarrow{G}$ [14]

$$\begin{aligned}
G_{x_px_q} &= \frac{-j\omega\mu_o k_o}{4\pi\alpha^3}e^{-j\alpha}[(\alpha^2 - 1 - j\alpha)\delta_{pq} \\
&\quad + (x_p - x'_p)(x_q - x'_q)(3 - \alpha^2 + 3j\alpha)/R^2] \\
\alpha &= k_oR, \quad R = |\vec{r} - \vec{r}'| \\
\vec{r} &= [x_1, x_2, x_3], \quad \vec{r}' = [x'_1, x'_2, x'_3].
\end{aligned} \tag{11}$$

Equations (9) and (10) can be converted into a matrix form. In the MoM computation, the volume integrals in (10) are computed by volume Gaussian quadrature integral method with six points each dimension. A cubic cell of edge length of 5 cm was used for modeling the human body. The wavelength is about 15 cm in the body tissue at 280 MHz. Thus, by using the six points Gaussian quadrature method, it results in subdividing the cubic cell into 216 subcells of edge length about 0.07 wavelength. The accuracy of the computation can

TABLE I
280-MHz NUMERICAL RESULTS OF THE INPUT IMPEDANCE, BODY-ABSORBED POWER, RADIATION EFFICIENCIES, AND POWER GAINS OF A SUPERQUADRIC LOOP ANTENNA IN FREE-SPACE OR APPROXIMATE TO A HUMAN-BODY MODEL AT THE CHEST POCKET AND WAIST BELT LEVELS

(Superquadric loop antenna : a=0.4 cm, b=2.25 cm, v=20, wire radius 0.08 cm. Human body muscle tissue : ε_r=54.5, σ=1.35 S/m)

Antenna Position	**In Free Space**	**Chest Pocket Level**			**Waist Belt Level**
Antenna Orientation	**Y**	**X**	**Y**	**Z**	**Y**
Input Impedance (Ω)	0.00362+j82.5	0.044+j82.5	0.0181+j82.5	0.0322+j82.5	0.0153+j82.5
Ohmic Loss Resistance (Ω)	0.0905	0.0905	0.0905	0.0905	0.0905
Radiation Efficiency $\eta_{r\Omega}$ (%)	4	33	17	26	14
Body-Absorbed Power (%)	0	87	60	73	55
Radiation Efficiency η_{rb} (%)	100	13	40	27	45
Total Radiation Efficiency* η_r (%)	4	4.29	6.8	7.02	6.3
Nosie Temperature** T_A (K)	296	267	283	274	286
E_θ Max. Power Gain in the H-Plane (dB)	-12.4	-14.1	-7.4	-16.0	-8.6
E_θ Min. Power Gain in the H-Plane (dB)	-22.3	-37.0	-56.8	-25.2	-34.0
E_θ Ave. Power Gain in the H-Plane (dB)	-15.0	-16.4	-13.6	-20.0	-13.4
E_ϕ Max. Power Gain in the H-Plane (dB)	<-100	-13.5	-20.8	-9.4	-21.3
E_ϕ Min. Power Gain in the H-Plane (dB)	<-100	-43.4	-38.5	-20.6	-41.3
E_ϕ Ave. Power Gain in the H-Plane (dB)	<-100	-17.0	-23.7	-12.4	-25.7
Computation Error (%)	0.76	1.42	0.6	0.99	1.0

* Total Radiation Efficiency $\eta_r = \eta_{r\Omega} \times \eta_{rb}$

** $T_A = \eta_{r\Omega} T_b + (1-\eta_{r\Omega}) T_p$; assuming T_b=200 K and T_p=300 K

be monitored by checking the antenna input power which should be equal to the sum of the radiation power (to free-space) and the body-absorbed power. It will be shown later (in Table I) the computation errors are lower than 1.5% for all cases used.

D. Antenna Radiation Characteristics Affected by the Body Absorption and Coupling Effects

The antenna current and the induced electric field inside the body can be determined by solving the above matrix equation. The antenna input impedance Z_i, input power (to the antenna) P_i, and radiation power absorbed by the body can then be calculated

$$Z_i = V_o/I_o, \quad P_i = \mathrm{Re}(V_o I_o^*)/2, \quad P_{\mathrm{abs}} = \int_{V_b} \frac{1}{2}\sigma|\vec{E}|^2\, dv. \tag{12}$$

The total radiation field (to free-space) is the sum of the radiation field from the loop antenna and the scattered field from the body. The radiation power to free-space can be calculated by integrating the radiation power density over a far-zone spherical surface and also the directive gain is then given by

$$P_{\mathrm{rad}} = \oint_s \frac{1}{2}\,\mathrm{Re}[\vec{E}^{\,r} \times \vec{H}^{r^*}] \cdot d\vec{s}$$

$$G(\theta,\phi) = \frac{\frac{1}{2}\,\mathrm{Re}(\vec{E}^{r} \times \vec{H}^{r^*})}{P_{\mathrm{rad}}/(4\pi r^2)}. \tag{13}$$

Since the antenna input power P_i should be equal to the sum of the body absorbed power P_{abs} and the radiation power P_{rad} (to free-space), these quantities can be used to check the EM coupling computation accuracy. The computation error is defined as

$$\text{computation error} = \frac{|P_i - (P_{\mathrm{rad}} + P_{\mathrm{abs}})|}{P_i}. \tag{14}$$

Two important quantities to evaluate human body effects on the radiation performance of the loop antenna are the radiation efficiency and the power gain. The antenna radiation pattern will be distorted by the body blocking effect and the antenna directive gain G will be significantly changed from that in free-space. There are two different antenna radiation efficiencies η_{rb} defined by the radiation power absorbed by the body and $\eta_{r\Omega}$ defined by the antenna ohmic loss

$$\eta_{rb} = \frac{P_{\mathrm{rad}}}{P_{\mathrm{rad}} + P_{\mathrm{abs}}} \quad \eta_{r\Omega} = \frac{R_r}{R_r + R_{\mathrm{ohm}}} \tag{15}$$

where R_r and R_{ohm} are the antenna radiation resistance and ohmic-loss resistance. The ohmic-loss resistance of a electrically small loop wire-antenna is given by

$$R_{\mathrm{ohm}} = \sqrt{\frac{\pi f \mu_o}{\sigma}}\left(\frac{\text{loop perimeter}}{2\pi r_i}\right) \tag{16}$$

where r_i is the wire radius and σ_c is the conductivity of the loop wire. Note that when the antenna is in free-space, there is no body-absorption effect and, hence, the η_{rb} is equal to one. The antenna power gain G_p and the average power gain G_{avg} can be obtained as

$$G_p = \eta_{rb} \times \eta_{r\Omega} \times G,$$

$$G_{\mathrm{avg}} = \frac{1}{8}\sum_{i=1}^{8} G_p\Big(\theta = \frac{\pi}{2}, \phi_i\Big), \quad \phi_i = i \times \frac{\pi}{4}. \tag{17}$$

The average power gain G_{avg} over the eight equal-angle positions in the H plane is appropriate for evaluating the antenna performance in wireless communications [7]. It is important to note that the power gain defined under the antenna ohmic loss and the body-absorption radiation efficiencies associated with (17) should be used to evaluate the antenna performance in the communication link budget. However, for the receiving

system analysis (such as S/N ratio), the antenna noise T_A is defined as [15], [16]

$$T_A = \eta_{r\Omega} T_b + (1 - \eta_{r\Omega}) T_p \tag{18}$$

where T_b is the background noise temperature and T_p is the antenna physical temperature. Only the ohmic-loss radiation efficiency is related. Two different radiation efficiencies should be used carefully in the receiving system analysis.

III. Numerical Results

Numerical simulations are conducted to ascertain the human-body effects on the loop antenna characteristics for some configurations of interest at 280-MHz VHF radio paging band. First, a rectangular loop with rounded corner in free-space is analyzed. Second, a realistically shaped 3-D man model with a height of 170 cm is constructed and used in the numerical simulations. Since the main interest is the effects of the proximate human body on the antenna radiation characteristics, the human body is modeled as a homogeneous muscle phantom with the relative permittivity $\varepsilon_r = 54.5$ and conductivity $\sigma = 1.35$ S./m at 280 MHz. The loop antenna may be located at the chest pocket level or the waist belt level of the human body.

A. Rectangular Loop Antenna with Rounded Corners in Free-Space

Consider a rounded corner rectangular loop in free-space that corresponds to a superquadric curve with parameters $a = 0.4$ cm, $b = 2.25$ cm, and $v = 20$. The wire radius is 0.08 cm and the loop perimeter is about 0.1λ at 280 MHz. It is of interest to discuss the convergence issue in numerical solutions. The number of the basis functions used to express the current distribution on the antenna surface is examined to ensure the accuracy of computed results. It can be found that 60 expansion functions would yield reasonably convergence result for the antenna input impedance. The 3-D linear-scale antenna patterns of E_θ and E_ϕ for x-, y-, and z-oriented loop are shown in Fig. 2. Note that the E_ϕ component is the dominant component for the z-oriented loop antenna, and the level of E_θ component is higher than that of E_ϕ for the x- and y-oriented loop.

B. Y-Oriented Loop Antenna at the Chest Pocket Level and the Belt Level of a Human Body

As shown in Fig. 1, a y-oriented loop antenna located at the chest pocket level ($d = 2$ cm, $w = 10$ cm, $h = 120$ cm) and at the waist belt level ($d = 2$ cm, $w = -10$ cm, $h = 100$ cm) is considered. The 3-D E_θ and E_ϕ patterns of the loop antenna affected by the human body are shown in Fig. 3. Fig. 4 shows the two-dimensional H-plane E_θ and E_ϕ power patterns, which include the body absorption and ohmic-loss effects [see (15)]. From these figures, it can be observed that due to the body blocking and absorption effects, the power gain of E_θ component will be much higher in the front direction than that in the backward direction of the human body. It is also noted that the cross-polarization field E_ϕ has been enhanced in the backward direction due to the body coupling effect.

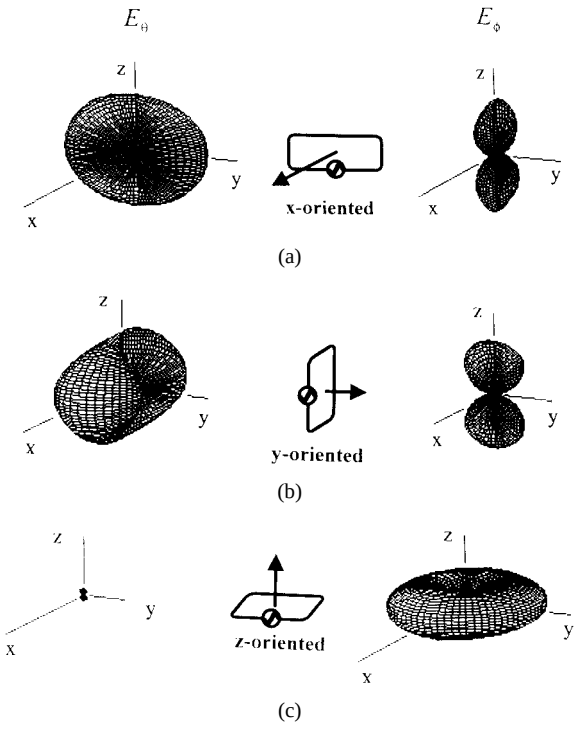

Fig. 2. Three-dimensional E_θ and E_ϕ patterns of a rectangular loop antenna in free-space at 280 MHz ($a = 0.4$ cm, $b = 2.25$ cm, wire radius $= 0.08$ cm, $v = 20$)). (a) x-oriented loop. (b) y-oriented loop. (c) z-oriented loop.

From the numerical results of the antenna current distribution, it is found that, while the imaginary part of the current has almost no change, the real part increases about five times for the chest pocket level and about three times for the belt level compared with that in free-space. The radiation resistance also increases about four to five times due to the body coupling effect (as shown in Table I). It is noted that the inductive reactance is much higher than the radiation resistance of the loop antenna (since the loop perimeter 0.1λ is electrically small). The enhancement of the radiation resistance by the human body represents a positive effect on radiation efficiency $\eta_{r\Omega}$ as defined in (15). The ohmic-loss resistance of the rectangular loop antenna is approximately 0.0905 Ω for the copper material $\sigma_c = 5.8 \times 10^7$ s/m. Thus, the radiation efficiency $\eta_{r\Omega}$ is 4% for the antenna in free-space, 17% at the chest pocket level, and 14% at the belt level. However, due to the body absorption effect, the radiation efficiency η_{rb} (which is 100% in free-space) is 40% for the chest pocket level and 45% for the belt level. Overall, the total radiation efficiency is 4% for the antenna in free-space, 6.8% at the chest pocket and 6.3% at the belt level. The average antenna power gain in the H-plane increases about 2 dB due to the body effects. This computed result is consistent with the previously reported data in [4].

C. Loop Antenna at Chest Pocket Level with Arbitrary Orientations

When the loop orientation changes from z axis to y axis, it corresponds to the Eulerian angles $\phi_w = 90^c$ and θ_w changes

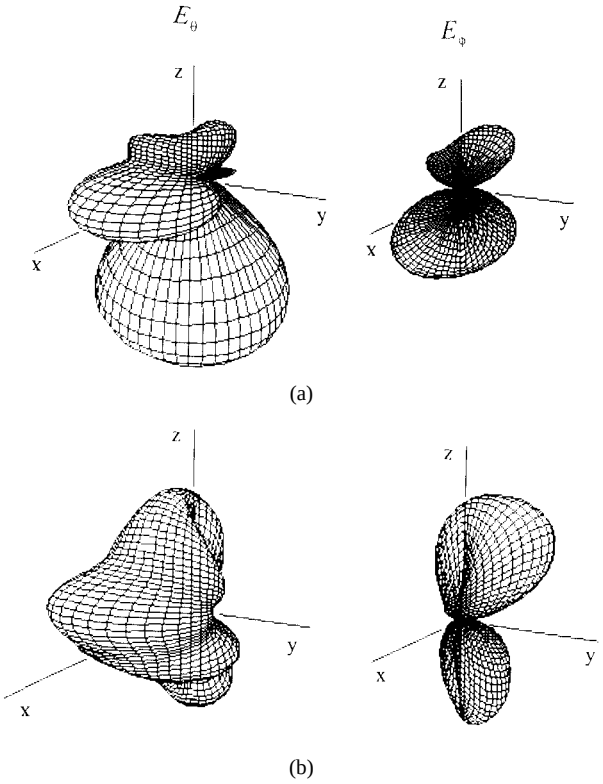

Fig. 3. Three-dimensional E_θ and E_ϕ patterns of a y-oriented rectangular loop antenna proximate to the human body at 280 MHz ($a = 0.4$ cm, $b = 2.25$ cm, wire radius $= 0.08$ cm, $v = 20$). (a) Chest pocket level. (b) Waist belt level.

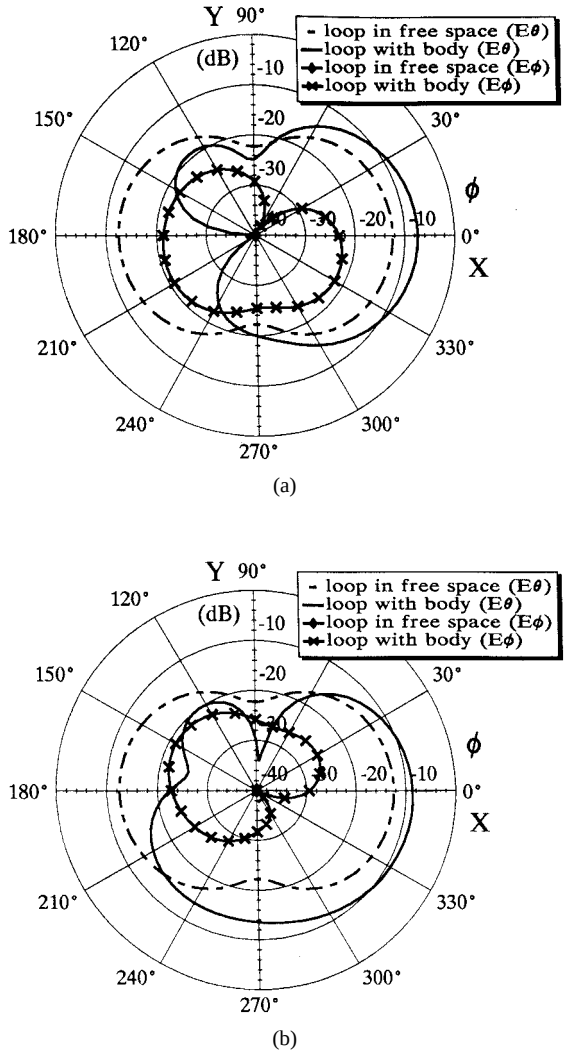

Fig. 4. Power patterns of E_θ and E_ϕ in the H-plane of a y-oriented rectangular loop antenna in free-space and proximate to a human body at 280 MHz ($a = 0.4$ cm, $b = 2.25$ cm, wire radius $= 0.08$ cm, $v = 20$). (a) Chest pocket level. (b) Waist belt level.

from 0° to 90°. If the loop orientation changes from z axis to x axis, then the Eulerian angles are $\phi_w = 0^c$ and θ_w from 0° to 90°. Fig. 5 shows the antenna efficiencies η_{rb} and $\eta_{r\Omega}$ versus the Eulerian angle θ_w. It can be observed that when the loop orientation moves from z axis to y axis, η_{rb} increases and $\eta_{r\Omega}$ decreases and, as that changes from z axis to x axis, η_{rb} decreases and $\eta_{r\Omega}$ increases. The increase of the antenna efficiency η_{rb} for the loop orientation changed from z axis to y axis can be explained as follows. To the z-oriented loop, the height of the body has a much longer "extension" than the width of the body in the y-oriented loop situation. Hence, the z-oriented loop will suffer more body absorption and has less radiation efficiency than the y-oriented loop. For the x-oriented loop, high body absorption is clear since the main radiation direction is aimed to the body. However, it is also observed that higher body absorption means more body coupling effect and more body enhancement to the antenna radiation resistance ,which increases the antenna efficiency $\eta_{r\Omega}$. This can also be seen in Fig. 6, which shows the antenna input impedance versus the Eulerian angle θ_w. The radiation resistance of the y-oriented loop antenna is the smallest and that of x-oriented loop is the highest. These characteristics are also depicted in Table I. Numerical results show that the loop antenna ohmic-loss efficiency increases from 4% (in free-space) to 33, 30, 26, 21, and 17% for the x-, xz- (z to x axis; $\theta_w = 45°$), z, zy (z to y axis; $\theta_w = 45°$), and y-oriented loops when proximate to the body (see Fig. 5). The radiation efficiencies, reduced by the body absorption effect, are 13, 18, 27, 26, and 40% for

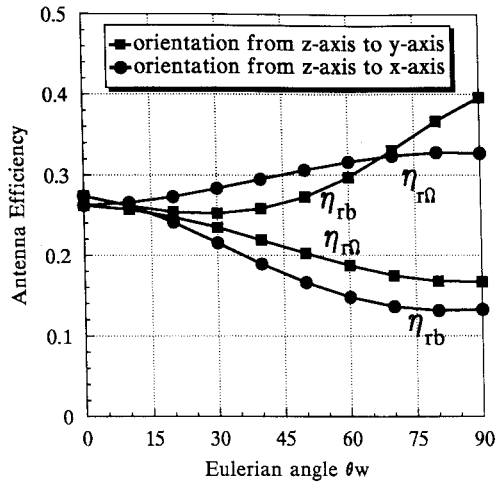

Fig. 5. Radiation efficiencies of a rectangular loop antenna (at the chest pocket level) versus the Eulerian angle θ_w at 280 MHz ($a = 0.4$ cm, $b = 2.25$ cm, wire radius $= 0.08$ cm, $v = 20$).

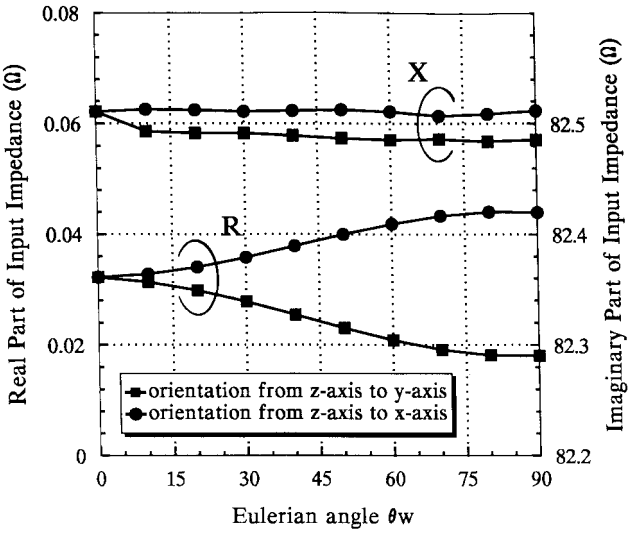

Fig. 6. Input impedance of a rectangular loop antenna (at the chest pocket level) versus the Eulerian angle θ_w at 280 MHz ($a = 0.4$ cm, $b = 2.25$ cm, wire radius $= 0.08$ cm, $v = 20$).

the x-, xz-, z-, zy-, and y-oriented loops, respectively. For the total antenna efficiency, the z- and y-oriented loop antennas have the higher value (about 7%).

To analyze these complicated power patterns and achieve important key values for wireless communications applications, the maximum, minimum, and average power gains of the E_θ and E_ϕ components (in the H plane) versus the Eulerian angle θ_w are computed and shown in Fig. 7 and are also listed Table I. For the E_θ field, the y-oriented loop has the highest values of the maximum and average power gain in the H-plane. While for the E_ϕ field, the maximum and average power gains of the z-oriented loop are the highest. These results are similar to the reported data in [8] for circular loop. Therefore, for vertical-polarization incident wave environment, the y-oriented loop antenna is the most suitable for the body-mounted pager usage. If the incident wave is horizontally polarized, the z-oriented loop antenna will be more suitable. Since in indoor or urban environments, both the vertical- and horizontal-polarization wave could exist, a good arrangement to combine the y- and z-oriented loops in a paging receiver may have a better receiving performance.

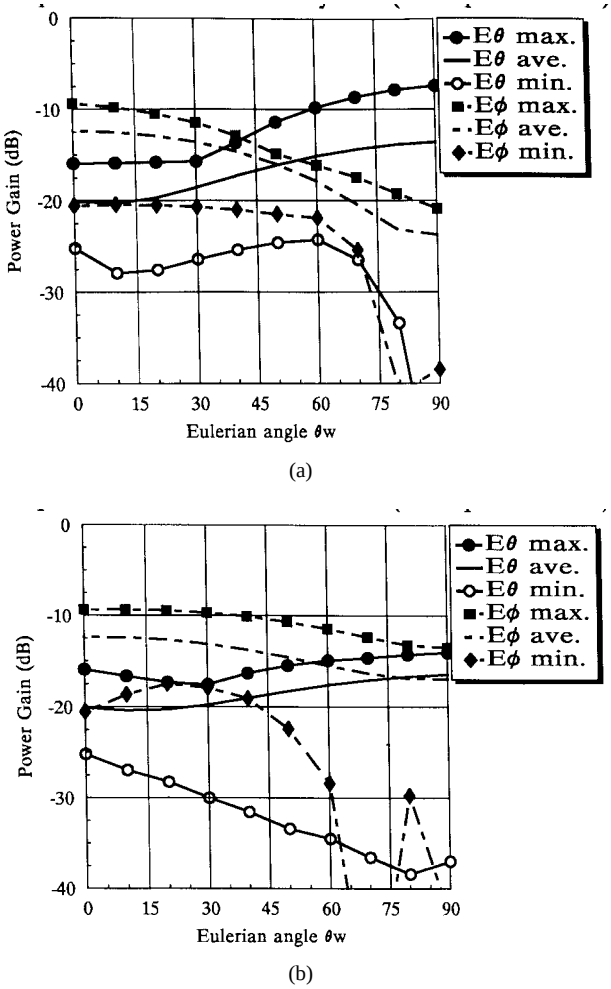

Fig. 7. E_θ and E_ϕ power gain in the H-plane of a rectangular loop antenna (at the chest pocket level) versus the Eulerian angle θ_w at 280 MHz ($a = 0.4$ cm, $b = 2.25$ cm, wire radius $= 0.08$ cm, $v = 20$). (a) Orientation from z axis to y axis. (b) Orientation from z axis to x axis.

IV. Summaries and Conclusions

In this paper, detailed analysis and extensive numerical simulation of the influence of a human-body model on an arbitrarily oriented loop antenna for personal wireless communications are presented. CIE, which consists of a PIE and a VEFIE with mutual coupling terms, and the MoM are used to numerically solve this antenna body coupling problem. A superquadric loop curve, which has the flexibility to model the circular, rectangular, and ellipse loop, is used to model the rectangular loop antenna with rounded corners. A magnetic frill source is used for the antenna feed modeling. The coordinate transformation technique is employed to allow the modeling of the loop antenna with arbitrary orientation. A 170-cm man model is constructed and a rounded corner rectangular loop antenna (0.8 cm $\times$ 4.5 cm) is used to simulate the internal loop antenna of a radio pager at 280-MHz VHF paging band. Numerical results show that the body coupling effect increases the ohmic-loss radiation efficiency of the loop antenna due to the enhancement of the radiation resistance (real part of the antenna input impedance). However, the radiation efficiency is reduced because a part of radiation power is absorbed by the human body. The ohmic-loss efficiency increases from 4% (in free-space) to 33, 30, 26, 21, and 17% when proximate to the body, and the body-absorption radiation efficiencies (100% in free-space) are 13, 18, 27, 26, and 40% for the x-, xz-, z-, zy-, and y-oriented loops, respectively. The power gain defined by the product of the directive gain, ohmic-loss efficiency, and body-absorption efficiency is an important quantity to evaluate the antenna performance influenced by the human body. The average power gain of the y-oriented loop antenna in the H-plane increases about 2 dB due to the body effects. Extensive numerical results for the loop antenna with various orientations are also presented to investigate the orientation effect of the loop with respect to the body. Computational results of loop antenna characteristics influenced by the human body are useful for the antenna/RF design and the link budget consideration of the personal communication systems.

REFERENCES

[1] J. Toftgard, S. N. Hornsleth, and J. Bach Andersen, "Effects on portable antennas of the presence of a person," *IEEE Trans. Antennas Propagat.*, vol. 41, pp. 739–746, June 1993.

[2] H.-R. Chuang, "Human operator coupling effects on radiation characteristics of a portable communication dipole antenna," *IEEE Trans. Antennas Propagat.*, vol. 20, pp. 556–560, Apr. 1994.

[3] M. A. Jensen and Y. Rahmat-Samii, "EM interaction of handset antennas and a human in personal communications," *Proc. IEEE*, vol. 83, pp. 1–17, Jan. 1995.

[4] Fujimoto and J. R. James, *Mobile Antenna Systems Handbook*. Norwood, MA: Artech House, 1994, ch. 4.

[5] K. Ito, I. Ida, and M.-shien Wu, "Body effect on characteristics of small loop antenna in pager systems," in *IEEE Antennas Propagat. Soc. Int. Symp. Dig.*, Chicago, IL, July 1992, vol. 2, pp. 1081–1084.

[6] J. S. Colburn and Y. Rahmat-Samii, "Electromagnetic scattering and radiation involving dielectric objects," *J. Electromagn. Waves Applicat.*, vol. 9, no. 10, pp. 1249–1277, Oct. 1995.

[7] K. Siwiak, *Radiowave Propagation and Antennas for Personal Communications*. Norwood, MA: Artech House, 1995, ch. 10.

[8] H.-R. Chuang and W.-T. Chen, "Computer simulation of the human-body effects on a circular-loop-wire antenna for radio-pager communications at 152, 280, and 400 MHz," *IEEE Trans. Veh. Technol.*, vol. 46, pp. 544–559, Aug. 1997.

[9] M. A. Jensen and Y. Rahmat-Samii, "Electromagnetic characteristics of superquadric wire loop antennas," *IEEE Trans. Antennas Propagat.*, vol. 42, pp. 264–269, Feb. 1994.

[10] ———, "Characterization of electromagnetically coupled superquadric loop antennas for mobile communications applications," *Proc. Inst. Elect. Eng.*, vol. 141, pt. H, no. 2, pp. 85–93, Apr. 1994.

[11] F. C. Chang, "Novel coordinate transformations for antenna applications," *IEEE Trans. Antennas Propagat.*, vol. AP-32, pp. 1292–1297, Dec. 1984.

[12] L. L. Tsai, "A numerical solution for the near and far fields of an annular ring of magnetic current," *IEEE Trans. Antennas Propagat.*, vol. AP-20, pp. 569–576, Sept. 1972.

[13] G. Zhou and G. S. Smith, "An accurate theoretical model for the thin-wire circular half-loop antenna," *IEEE Trans. Antennas Propagat.*, vol. 39, pp. 1167–1177, Aug. 1991.

[14] D. E. Livesay and K.-M. Chen, "Electromagnetic fields induced inside arbitrarily shaped biological bodies," *IEEE Trans. Microwave Theory Tech.*, vol. 22, pp. 1273–1280, Dec. 1974.

[15] D. M. Pozar, *Microwave Engineering*. Reading, MA: Addison-Wesley, 1990, ch. 12.

[16] C. A. Balanis, *Antenna Theory: Analysis and Design*. New York: Wiley, 1997, ch. 2.

Wen-Tzu Chen (S'97) was born in Kaohsiung, Taiwan, R.O.C., on December 24, 1965. He received the B.S.E.E. degree from the National Cheng Kung University, Tainan, Taiwan, and the M.S.E.E. degree from the National Taiwan University, Taipei, Taiwan, in 1987 and 1989, respectively. He is currently working toward the Ph.D. degree at the Department of Electrical Engineering, National Cheng Kung University, Tainan, Taiwan.

From 1991 to 1992, he was a Lecturer in the Chung Hwang Technical Junior College, Taipei, Taiwan. In 1992 he joined the Victory Industrial Corp., Hsi-Chih, Taiwan, as a Microwave Engineer. From 1993 to 1995 he was with the Educational Broadcasting Station, Kaohsiung, Taiwan, as an RF Supporting Engineer. His research interests include numerical computation of electromagnetic interaction between the antenna and the human body and microwave antenna design.

Huey-Ru Chuang (M'97) was born in Tainan, Taiwan, R.O.C., on August 18, 1955. He received the B.S.E.E. and M.S.E.E. degrees from the National Taiwan University, Taipei, Taiwan, in 1977 and 1980, respectively, and the Ph.D. degree in electrical engineering from Michigan State University, East Lansing, in 1987.

From 1987 to 1988, he was a Postdoctoral Research Associate at the Engineering Research Center, Michigan State University. From 1988 to 1990 he was with the Portable Communication Division, Motorola Inc., Ft. Lauderdale, FL. Since 1991 he has been an Associate Professor with the Department of Electrical Engineering, National Cheng Kung University, Tainan, Taiwan. His research interests include electromagnetic computation of the interaction between the antenna and the human body, portable antenna design for wireless communications, satellite reflector antennas, EMI/EMC measurements and modeling, RF/microwave communication circuits design, and microwave detection systems.